PERGAMON

International Journal of Heat and Mass Transfer 45 (2002) 3839–3847

International Journal of HEAT and MASS TRANSFER

www.elsevier.com/locate/ijhmt

A two-dimensional fin efficiency analysis of combined heat and mass transfer in elliptic fins

Chien-Nan Lin, Jiin-Yuh Jang *

Department of Mechanical Engineering, National Cheng-Kung University, Tainan 70101, Taiwan, ROC

Received 26 June 2001; received in revised form 28 December 2001

Abstract

This paper presents a two-dimensional analysis for the efficiency of an elliptic fin under the dry, partially wet and fully wet conditions of a range of value for axis ratios, Biot numbers, and air humidifies. It is shown that the fin efficiencies increase as the axis ratio Ar is increased. For a given axis ratio Ar, the fin efficiency decreases as the fin height l^* or Biot number is increased. The conventional 1-D sector method overestimates the fin efficiency resulting in increasing error as the axis ratio Ar is increased. In addition, using experimentally determined heat transfer coefficients, it is found that both the fully dry and wet elliptic fin efficiencies are up to 4–8% greater than the corresponding circular fin efficiencies having the same perimeter.

Keywords: Fin efficiency; Elliptic fins; Heat and mass transfer

1. Introduction

Finned tubes are widely used in the industrial heat exchangers, especially for air-cooling and dehumidification. The effectiveness of the heat exchanger primarily depends on the efficiency of the fin attached to the tube. If the temperature of entire fin surface is higher than the dew point of the surrounding air, there is only sensible heat transferred from the air to the fin and so the fin is fully dry. If the temperature of the entire fin surface is below the dew point and both the sensible and latent heat are produced, the fin becomes fully wet. The fin is partially wet if the fin base temperature is lower than the dew point while the fin tip temperature is higher than the dew point of the surrounding air. Depending on applications and design criteria, the shapes of tubes and fins have many possibilities. One type of heat exchanger, is that constructed of circular pipes with circular fins or continuous plate fins which has been used in many industries. An elliptic cylinder is a common form, which could take the shape of a flat plate or a circular cylinder depending upon the major to minor axes ratio. There may be an advantage when using elliptic tubes with elliptic fins as the pumping power needed to flow fluids around the tube is reduced. The disadvantage is that the elliptic tubes are generally restricted to low-pressure applications in the tube side.

For fully dry rectangular and circular fins, most of the widely used heat transfer texts or handbooks, such as McQuiston and Parker [1] and ARI Standard 410-72 [2], provide the fin efficiency equations. For fully wet fins, Threlkeld [3] and McQuiston [4] obtained analytical expressions for the one-dimensional (1-D) fin efficiency of a rectangular fin, where the calculation of wet fin efficiency is based on a modified dry fin formula. It was shown that the wet fin efficiency is lower than that of a dry fin. Coney et al. [5,6] numerically analyzed the 1-D fully wet fin efficiency for a rectangular fin, where the variations of film thickness and local mass transfer effect are considered. Kazeminejad [7] presented a 1-D conjugate forced convection–conduction analysis of the performance of a fully wet rectangular fin assembly. Chen [8] developed a two-dimensional (2-D) numerical model of a fully wet rectangular fin. The results of 2-D model vary significantly, especially at low relative humidity, from those of the traditional 1-D model. The analytical and numerical solutions for fully wet 1-D

* Corresponding author. Tel.: +86-6-2757575x62148; fax: +886-6-2753850.

E-mail address: jangjim@mail.ncku.edu.tw (J.-Y. Jang).

0017-9310/02/$ - see front matter
PII: S0017-9310(02)00086-8

Nomenclature

A	area of fin surface (mm^2)
Ar	axis ratio of elliptic tube, a/b
a	semi-major axis of elliptic tube (mm)
b	semi-minor axis of elliptic tube (mm)
Bi	Biot number, $Bi = hb/k$
c_1	constant defined in Eq. (6)
c_2	constant defined in Eq. (6) ($°C^{-1}$)
c_3	constant defined in Eq. (6) ($°C^{-2}$)
c_p	specific heat of dry air (kj kg^{-1} $°C^{-1}$)
h	average heat convective coefficient on the air side (W m^{-2} $°C^{-1}$)
h_d	average mass transfer coefficient based on the humidity ratio difference (kg m^{-2} s^{-1})
i	enthalpy of moist air (kj kg^{-1})
i_{fg}	latent heat of evaporation of water (kj kg^{-1})
k	thermal conductivity of fin (W m^{-1} $°C^{-1}$)
Le	Lewis number, $Le = (h/h_d c_p)^{3/2}$
l	fin height (mm)
l^*	dimensionless fin height, $l^* = l/b$
n	normal direction of elliptic fin edge (mm)
q	heat transfer rate (W)
r	radius distance of fin (mm)
S	edge of the elliptic fin
T	temperature (°C)
V	air velocity (m s^{-1})
W	humidity ratio of saturated air at T (kg water vapor/ kg dry air)
W_a	humidity ratio of ambient air (kg water vapor/ kg dry air)
X	x/b dimensionless coordinate
Y	y/b dimensionless coordinate

Greek symbols

δ	fin thickness (mm)
δ^*	dimensionless fin thickness, $\delta^* = \delta/b$
η	fin efficiency
Θ	dimensionless temperature $\Theta = (T - T_a)/(T_b - T_a)$
φ	relative humidity

Subscripts

a	air
b	fin base
dew	dew point temperature
dry	dry fin
fin	fin surface
wet	wet fin

circular fins have been reported by various investigators, such as Elmahdy and Biggs [9], Hong and Webb [10], Wang et al. [11] and Rosario and Rahman [12]. Recently, Liang et al. [13] investigated the 1-D and 2-D wet-surface efficiency of a plate-fin-tube heat exchanger. The 2-D model takes into account of the complex fin geometry and the variation of the moist air properties over the fin.

For the partial wet condition, Wu and Bong [14] and Salah El-Din [15] provided the 1-D analytical solutions for the fin efficiencies of rectangular fin and fin assembly, respectively, under both partially wet and fully wet conditions. Rosario and Rahman [16] presented the 1-D analysis of heat transfer in a partially wet circular fin assembly during dehumidification. Besendnjak and Poredos [17] analyzed the 3-D computational fluid dynamics analysis of turbulent heat and mass transfer between the moist air and a rectangular fin.

For elliptic fin, Brauer [18] was the first author to study the thermal-characteristics of an elliptic finned-tube heat exchanger having an axis ratio of 1.77:1 under only the dry condition. Jang and Yang [19] presented the thermal-hydraulic characteristics of a 4 row elliptic finned-tube heat exchanger under the dry and dehumidifying conditions for two elliptic finned-tube heat exchangers with staggered and in-lined arrangements and having an axis ratio of 2.83:1, fin height 7 mm and fin pitch 8 fins/in., respectively. For the dry conditions, the average heat transfer coefficient of elliptic finned-tube is 35–50% that of the corresponding circular finned-tube, while the pressure drop for an elliptic finned-tube bank is only 25–30% that of the circular one. For the dehumidifying conditions, the sensible j_s factor for the wet coils is 20–30% higher than that of the j factor for the dry coil while the wet friction factor is 10–25% higher than that of the dry coils; the mass transfer Colburn j_t factor for an elliptic finned-tube is 30–40% lower than that of the corresponding circular finned-tube. Since there was no analytical solution for the dry or wet fin efficiency of an elliptic fin and therefore the elliptic fin efficiency in [19] was calculated by using the sector method [20], with 200 sectors and the fin efficiencies for each small sector obtained from the 1-D dry and fully wet circular fin formula. Rocha et al. [21] used a 2-D numerical model to study one- and two-row circular and elliptic tubes and plate fin heat exchangers to compare the dry fin efficiency of the two configurations. A relative fin efficiency gain of up to 18% was observed by the elliptical arrangement. Recently, Saboya and Saboya [22] provided the experimental results for average heat transfer coefficients in a rectangular plate fin and elliptical tube heat exchangers with one and two rows using naphthalene sublimation technique.

The foregoing literature review shows that no related work on the 2-D analysis for the efficiency of an elliptic fin under the dry, partially wet and fully wet conditions has been previously published. This has motivated the present investigation.

2. Mathematical analysis

The physical model of the elliptic fin-tube heat exchanger is shown in Fig. 1, where a and b are the lengths of the semi-major and minor axes of the elliptic tube, respectively, l is the fin height and δ is the fin thickness. The following assumptions were made to complete the development of the theoretical model:

1. The surface temperature of the elliptic tube, T_b, is considered to be constant.
2. Both the convective heat transfer coefficient, h, and the mass transfer coefficient, h_d, are constant.
3. The thermal conductivities of the fin, k, are constant.
4. Condensation occurs when the fin temperature T is below the dew point of the moist air T_{dew}.
5. The thermal contact resistance between the tube and the fin is negligible and the condensate film is very thin.
6. Due to the thin fin behavior, the temperature gradient in the z direction (fin thickness) is very small and fin temperature varies only in the x and y directions, i.e., $T(x,y)$.

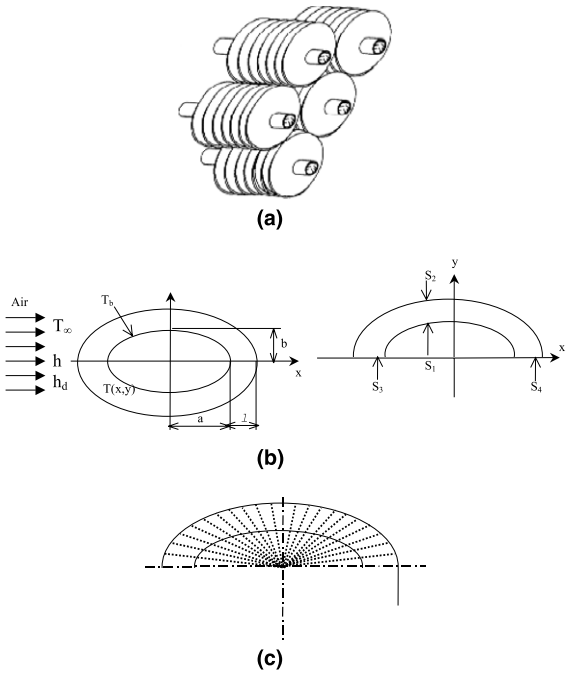

Fig. 1. The physical model and coordinate system: (a) elliptic fin-tube heat exchanger; (b) elliptic fin-tube section geometry and coordinate system; (c) conventional sector method for the elliptic fin.

2.1. Governing equations

The governing differential equations for the 2-D temperature distribution can be derived as follows:

Dry fin

$$\frac{\partial^2 T}{\partial x^2}+\frac{\partial^2 T}{\partial y^2}=2\frac{h}{k\delta}(T-T_a). \tag{1}$$

Fully wet fin

$$\frac{\partial^2 T}{\partial x^2}+\frac{\partial^2 T}{\partial y^2}=\frac{2h}{k\delta}(T-T_a)+\frac{2h_d}{k\delta}(W-W_a)i_{fg}. \tag{2}$$

Partially wet fin

$$\frac{\partial^2 T}{\partial x^2}+\frac{\partial^2 T}{\partial y^2}=2\frac{h}{k\delta}(T-T_a)$$
$$\text{for dry domain } (T>T_{dew}), \tag{3}$$

$$\frac{\partial^2 T}{\partial x^2}+\frac{\partial^2 T}{\partial y^2}=\frac{2h}{k\delta}(T-T_a)+\frac{2h_d}{k\delta}(W-W_a)i_{fg}$$
$$\text{for wet domain } (T<T_{dew}), \tag{4}$$

where the h_d is the average mass transfer coefficient based on the humidity ratio difference, W is the humidity ratio of saturated air at temperature T, W_a is the humidity ratio of the atmospheric air, and i_{fg} is the latent heat of condensation.

On introducing the following dimensionless variables and parameters:

$$X=x/b,\quad Y=y/b,\quad l^*=l/b\quad \delta^*=\delta/b,$$
$$\Theta=\frac{T-T_a}{T_b-T_a},\quad Bi=\frac{hb}{k},\quad Ar=\frac{a}{b},\quad Le=\left(\frac{h}{h_d c_p}\right)^{3/2}, \tag{5}$$

where Bi is the Biot number and Ar is the axis ratio of the elliptic tube; Le is the Lewis number, and for atmospheric air Le is about equal to 0.854 from 10 °C to 32 °C [1]. In addition, from the regression analysis, the relationship between the saturated water film temperature T and the corresponding saturated humidity ratio W can be approximated by the following second order polynomial equation:

$$W=c_1+c_2T+c_3T^2, \tag{6}$$

where $c_1=0.00378$, $c_2=0.000209$ ($^\circ C^{-1}$), $c_3=0.000018$ ($^\circ C^{-2}$) for $0\,^\circ C\leqslant T\leqslant 30\,^\circ C$, and the error for Eq. (6) is less than 3% as compared with the Psychometric chart.

Eqs. (1)–(4) can be nondimensionalized as follows:

Dry fin

$$\frac{\partial^2\Theta}{\partial X^2}+\frac{\partial^2\Theta}{\partial Y^2}=2Bi\frac{1}{\delta^*}\Theta. \tag{7}$$

Fully wet fin

$$\left(\frac{\partial^2\Theta}{\partial X^2}+\frac{\partial^2\Theta}{\partial Y^2}\right)=2Bi\frac{1}{\delta^*}\left\{\frac{i_{fg}}{(Le)^{2/3}c_p}c_3(T_b-T_a)\Theta^2+\left[\frac{i_{fg}}{(Le)^{2/3}c_p}(2c_3T_a+c_2)+1\right]\Theta+\left[\frac{i_{fg}}{(Le)^{2/3}c_p}\frac{c_1+c_2T_a+c_3T_a^2-W_a}{T_b-T_a}\right]\right\}. \tag{8}$$

Partially wet fin

$$\frac{\partial^2\Theta}{\partial X^2}+\frac{\partial^2\Theta}{\partial Y^2}=2Bi\frac{1}{\delta^*}\Theta \quad \text{dry domain } \Theta>\Theta_{dew}, \tag{9}$$

$$\left(\frac{\partial^2\Theta}{\partial X^2}+\frac{\partial^2\Theta}{\partial Y^2}\right)=2Bi\frac{1}{\delta^*}\left\{\frac{i_{fg}}{(Le)^{2/3}c_p}c_3(T_b-T_a)\Theta^2+\left[\frac{i_{fg}}{(Le)^{2/3}c_p}(2c_3T_a+c_2)+1\right]\Theta+\left[\frac{i_{fg}}{(Le)^{2/3}c_p}\frac{c_1+c_2T_a+c_3T_a^2-W_a}{T_b-T_a}\right]\right\}$$

$$\text{wet domain } \Theta\leqslant\Theta_{dew}. \tag{10}$$

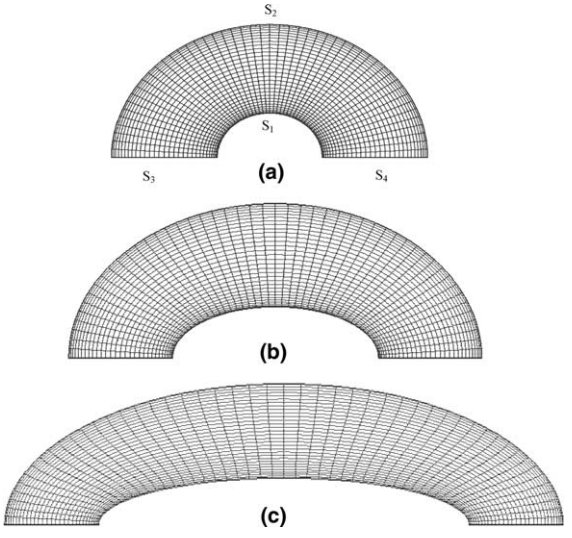

Fig. 2. Computational domain of elliptic fin for different aspect ratio: (a) $Ar=1$, (b) $Ar=2$, (c) $Ar=4$.

2.2. Boundary conditions

The boundary conditions for the 2-D thin fin energy equations are

$$\text{at } S_1, \quad \Theta=1,$$

$$\text{at } S_2,\ S_3 \text{ and } S_4 \quad \frac{\partial\Theta}{\partial n}=0. \tag{11}$$

At the base of the elliptic fin (S_1), an isothermal condition is used. At the fin tip (S_2), the heat and mass transfer from the fin tip to the surrounding air is assumed to be negligible due to its very small fin thickness. Since the elliptic fin-tube is symmetric along the major axis (S_3 and S_4), the temperature gradient is zero. In dew point of the surrounding air.

2.3. Fin efficiency

The fin efficiency is defined as the ratio of actual total heat transfer rate to the maximum total heat transfer rate, as in $\eta=q_{actual}/q_{maximum}$, i.e.

Dry fin

$$\eta_{dry}=\frac{q_{T=T_{fin}}}{q_{T=T_b}}=\frac{\int(T_a-T)\,dA}{\int(T_a-T_b)\,dA}=\frac{\int\Theta\,dA}{\int dA}. \tag{12}$$

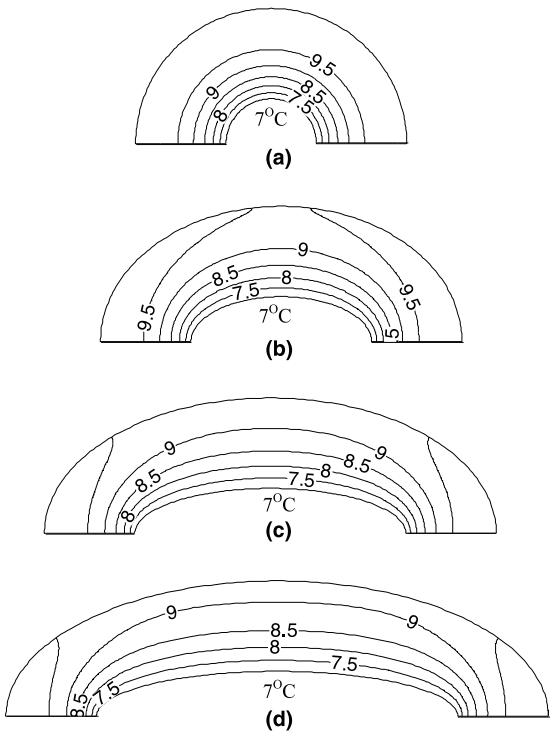

Fig. 3. The temperature profile of dry fin for different aspect ratio at $Bi=1.67\times10^{-3}$, $I^*=2.0$, $\overline{\delta}=0.06$, $T_a=27$ °C, $T_b=7$ °C. (a) $Ar=1$, (b) $Ar=2$, (c) $Ar=3$, (d) $Ar=4$.

Fully wet fin

$$\eta_{\text{wet}} = \frac{\int [c_p(T_a - T) + \frac{1}{(Le)^{2/3}}(W_a - W) i_{fg}]\, dA}{\int [c_p(T_a - T_b) + \frac{1}{(Le)^{2/3}}(W_a - W_b) i_{fg}]\, dA}. \quad (13)$$

Partially wet fin

The fin efficiencies for the fully dry and wet regions can be calculated separately from Eqs. (12) and (13). It can be shown that the partially wet fin efficiency for the entire fin is

$$\eta_{\text{partial wet}} = \frac{A_{\text{dry}}}{A}\eta_{\text{dry}} + \frac{A_{\text{wet}}}{A}\eta_{\text{wet}}, \quad (14)$$

where A_{dry} and A_{wet} are the surface area for the dry and wet regions, respectively.

3. Numerical analysis

The governing equations (7)–(10) together with the boundary conditions (11) were solved numerically. The 2-D elliptic partial differential equations are expressed in the finite difference forms by a second-order central difference scheme. A grid system of 151×101 grid points is typically adopted in the computation domain as shown in Fig. 2 However, a careful check of the grid-independence for the numerical solutions has been made to ensure the accuracy and validity of the numerical results. For this purpose, three grid systems, 81×51, 151×111 and 301×221, are tested. It is found that for axis ratio $Ar = 4$, $T_a = 27$ °C, $T_b = 7$ °C, $\delta = 80\%$, the relative errors in the local temperature between the solutions of 151×111 and 301×221 are less than 1%.

The numerical computations were started by first estimating the temperature distributions in the whole fin domain and then solving the finite difference algebraic equations iteratively until the converged solutions were obtained. The convergence criterion is satisfied when the relative errors of temperatures are less than 1.0×10^{-6}. It is noted that for a partially wet fin, the temperatures in the entire fin surface were checked in each iteration to decide whether the dry fin equation (9) or wet fin equation (10) should be used.

4. Results and discussion

Figs. 3(fully dry) and 4(fully wet) show the temperature distributions, for different axis ratio ($Ar = 1, 2, 3$ and 4) under the following operation conditions:

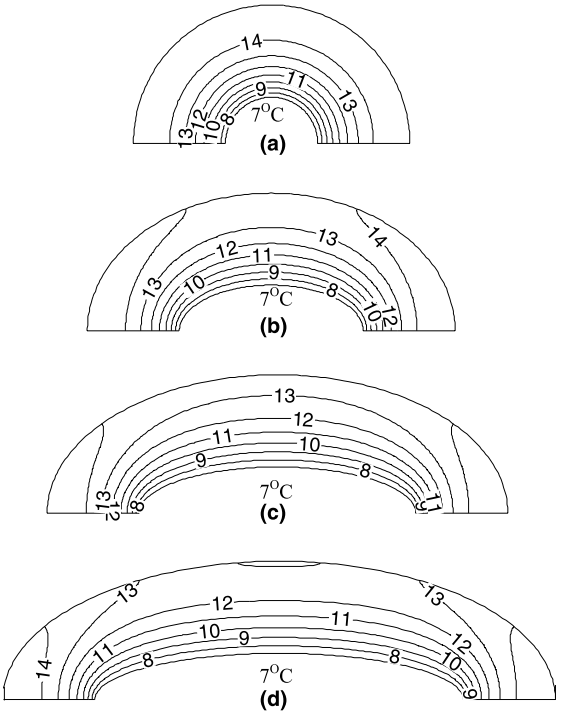

Fig. 4. The temperature profile of fully wet fin for different aspect ratio at $Bi = 1.67 \times 10^{-3}$, $l^* = 2.0$, $\overline{\delta} = 0.06$, $\phi = 80\%$, $T_a = 27$ °C, $T_b = 7$ °C. (a) $Ar = 1$, (b) $Ar = 2$, (c) $Ar = 3$, (d) $Ar = 4$.

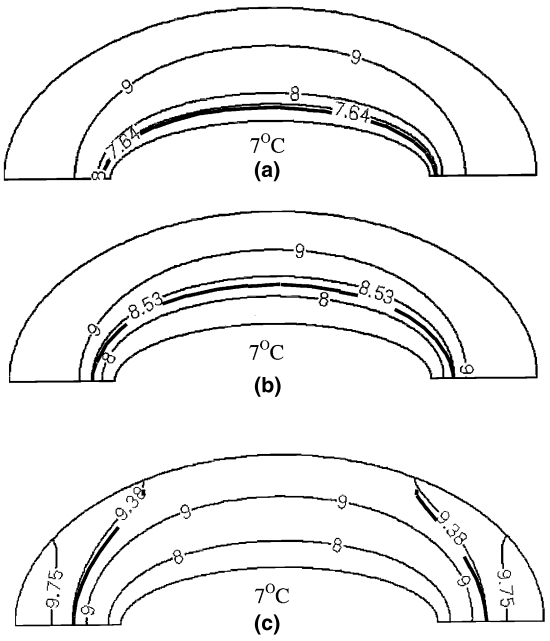

Fig. 5. The dry-wet interface and temperature distribution for different inlet air humidity: (a) $\phi = 29\%$ ($T_{\text{dew}} = 7.64$ °C); (b) $\phi = 31\%$ ($T_{\text{dew}} = 8.53$ °C); (c) $\phi = 33\%$ ($T_{\text{dew}} = 9.38$ °C) at $T_a = 27$ °C, $T_b = 7$ °C, $Bi = 1.67 \times 10^{-3}$, $l^* = 2$ and $\overline{\delta} = 0.006$, $Ar = 3$.

ambient air temperature $T_a = 27$ °C, relative humidity $\phi = 80\%$ (fully wet fin), fin base temperature $T_b = 7$ °C, $l^* = 2.0$, $\delta^* = 0.06$ and $Bi = 1.67 \times 10^{-3}$. It is noted that $Ar = 1.0$ corresponds to the case of a circular fin, in which the 1-D analytical solutions for the fully dry [1] and fully wet solutions [11] are available. It is seen that the temperature profiles are indeed two-dimensional for elliptic fins. The temperature gradients in the regions adjacent to the minor axis are smaller than those of regions near the major axis. It is also observed that due to additional latent heat transfer from the moist air ($\phi = 80\%$) to the fin, the temperatures of a fully wet fin are higher than those for a fully dry fin. Figs. 5(a)–(c) illustrate the temperature distribution of a partial wet fin with an axis ratio $Ar = 3.0$ for three different air relative humidity $\phi = 29\%$, 31% and 33%, respectively, for $T_a = 27$ °C, $T_b = 7$ °C, $l^* = 2.0$, $\delta^* = 0.06$ and $Bi = 1.67 \times 10^{-3}$. The corresponding dew point temperatures for $\phi = 29\%$, 31% and 33% are 7.64 °C, 8.53 °C and 9.38 °C, respectively, and are also shown in the figure to indicate the interface of the fully dry and wet regions. As expected, the fin temperature distribution is higher as the air relative humidity ϕ is increased because more latent heat is transferred from the moist air to the fin surface. In addition, as ϕ is increased, the interface of the fully dry and wet regions moves outward to the elliptic fin tip resulting in the increase of the wet region.

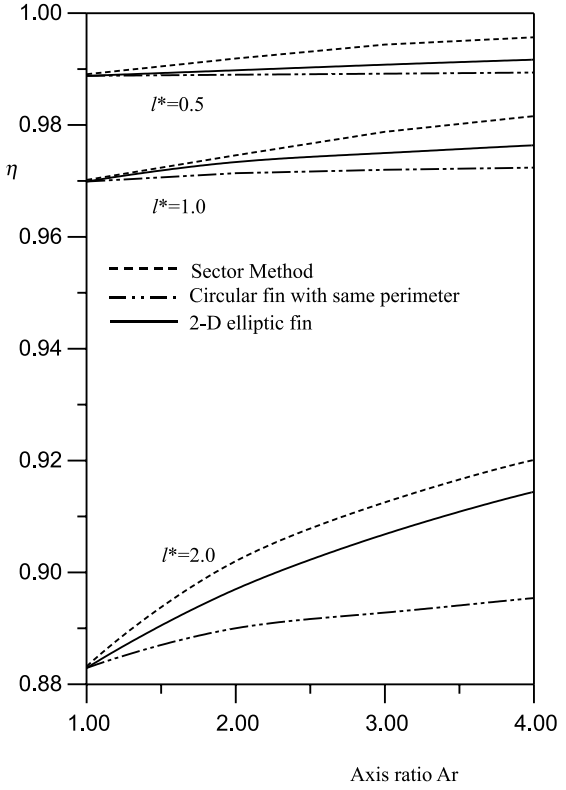

Fig. 6. The variations of fully dry fin efficiency as function of Ar for different values of fin height l^* under $T_a = 27$ °C, $T_b = 7$ °C, $Bi = 1.67 \times 10^{-3}$ and $\delta^* = 0.06$.

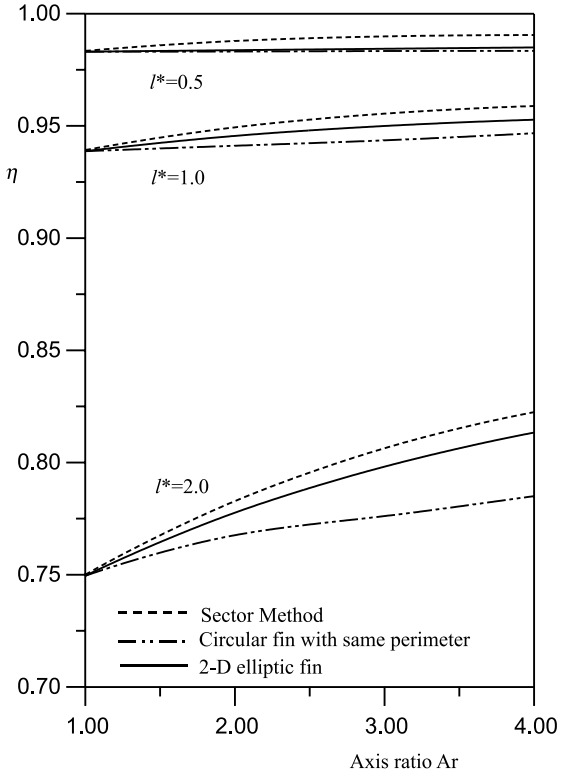

Fig. 7. The variations of fully wet fin efficiency as function of Ar for different values of fin height l^* under $T_a = 27$ °C, $\phi = 80\%$, $T_b = 7$ °C, $Bi = 1.67 \times 10^{-3}$ and $\delta^* = 0.06$.

Figs. 6 and 7 present the variations of fully dry and wet fin efficiencies, respectively, as a function of axis ratio Ar, ranging from 1.0 to 4.0, for different values of fin height ($l^* = 0.5$, 1.0 and 2.0), under the conditions of $T_a = 27$ °C, $\phi = 80\%$, $T_b = 7$ °C, $Bi = 1.67 \times 10^{-3}$ and $\delta^* = 0.06$. It is shown that the both the fully dry and wet fin efficiencies are increased as the axis ratio Ar is increased, and the fully wet fin efficiency is 10–20% lower than that of a dry fin. For a given axis ratio Ar, the fin efficiency decreases as the fin height l^* is increased. The dashed lines denote the conventional sector method with 50 sectors, and the fin efficiencies for each small sector were obtained using the 1-D dry [1] and wet [11] circular fin formula. The numerical results indicated that the conventional 1-D sector method overestimates the fin efficiency, resulting in increasing error as the axis ratio Ar is increased. For example, for $Ar = 2.0$, the 1-D sector method overestimates the elliptic fully dry and

wet fin efficiencies by 0.5%, while for $Ar = 4.0$, the 1-D sector method overestimates the fully dry and wet efficiencies by 1% as compared to the 2-D analysis. Since the elliptic tube is usually made from the circular tube having the same perimeter, the corresponding 1-D circular dry and wet fin efficiencies of elliptic fin are also shown for comparison. The numerical results indicate that the both the dry and wet elliptic fin efficiencies are 1–4% higher than the corresponding circular fin efficiencies having the same Biot number (or heat transfer coefficient).

The variations of the fin efficiency as a function of the air relative humidity over the full range of $\phi = 0\%$ to $\phi = 100\%$, for two different values of fin height l^* ($l^* = 1.0$ and $l^* = 2.0$) and Biot numbers ($Bi = 1.67 \times 10^{-3}$ and 3.33×10^{-3}), are illustrated in Figs. 8 and 9, respectively, under the conditions of $T_a = 27$ °C, $T_b = 7$ °C and $\delta^* = 0.06$. Similar to the 1-D results found for a rectangular fin [1] or a circular fin [11], as the air relative humidity varies from $\phi = 0\%$ to $\phi = 27.3\%$ the fin is fully dry because the corresponding dew point temperatures are below 7 °C. Therefore the fin efficiency is independent of ϕ and remains constant. When $27.3\% < \phi < 40\%$, the fin is in a partially wet situation; the fin efficiency is reduced rapidly as the air relative humidity increases. When $\phi > 40\%$, the fin is fully wet, and the fin efficiency is only slightly dependent on the air relative humidity.

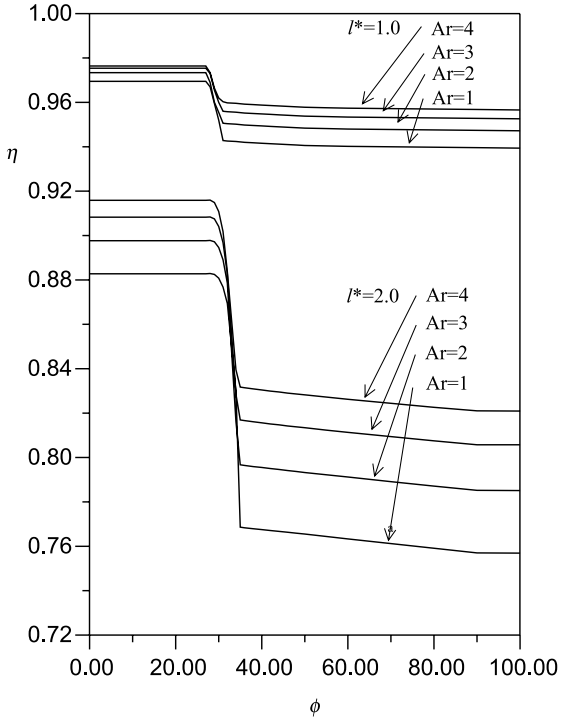

Fig. 8. The variations of fin efficiency as a function ϕ for two different values of fin height l^* under the case of $T_a = 27$ °C, $T_b = 7$ °C, $Bi = 1.67 \times 10^{-3}$ and $\delta^* = 0.06$.

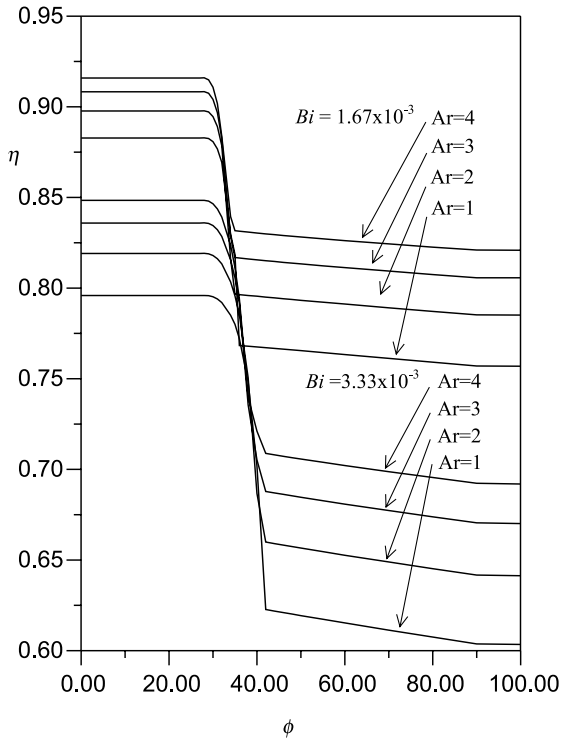

Fig. 9. The variations of fin efficiency as a function ϕ for two different values of Bi under the case of $T_a = 27$ °C, $T_b = 7$ °C, $l^* = 2$ and $\delta^* = 0.06$.

Finally, it is interesting to compare the fin efficiency as a function of air velocity between the elliptical fin and the corresponding circular fin using the experimentally determined heat transfer and mass transfer coefficients from Jang and Yang [19]. The lengths of the major and minor axes for the elliptic tube used in [19] are 36×12.7 mm ($Ar = 2.83$), and the diameter of the corresponding circular fin tube is 27.2 mm. The fin height is 7 mm and fin pitch 8 fins/in. The average heat and mass transfer and coefficients of elliptic finned-tube are 35–50% (dry condition), 30–40%, (wet condition), lower than that of the corresponding circular finned-tube. Figs. 10 and 11 illustrate the variations of the fully dry and wet fin efficiencies, respectively, as function of various inlet front air velocities ranging from 1.5 to 6 m/s for two different fin materials (aluminum and carbon steel). As expected, both the fully dry and wet fin efficiencies decrease as the frontal velocity increases due to the increase of the average heat or mass transfer coefficient. A closer look at the figures indicates that the elliptic fin efficiency is up to 4% higher than the corresponding circular fin efficiencies

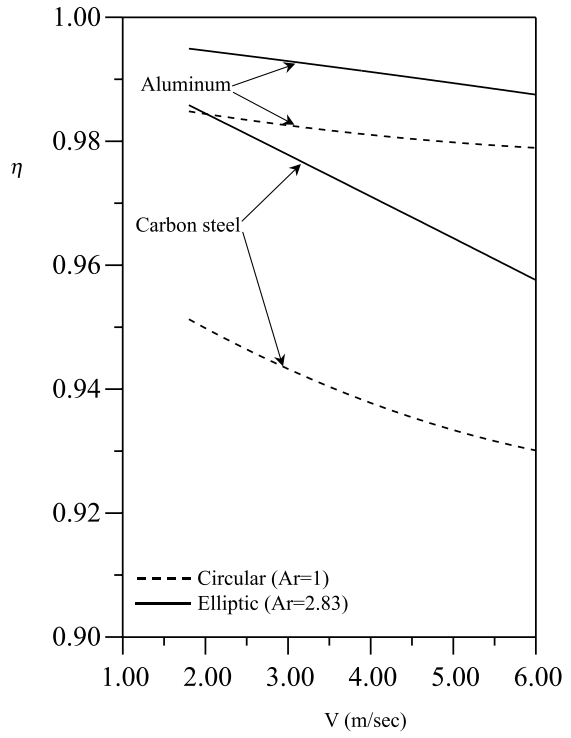

Fig. 10. The fully dry fin efficiencies as function of various inlet front air velocities for two different fin materials using the experimentally determined heat transfer coefficients from Jang and Yang [19].

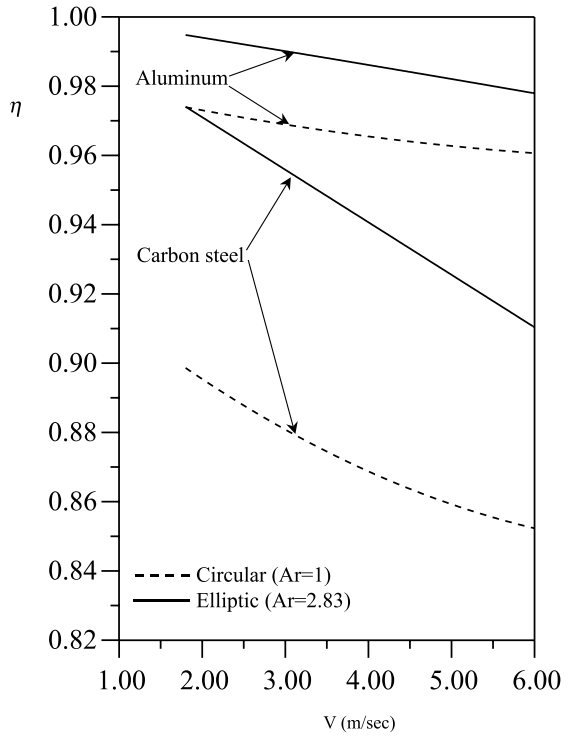

Fig. 11. The fully wet fin efficiencies as function of various inlet front air velocities for two different fin materials using the experimentally determined heat and mass transfer coefficients from Jang and Yang [19].

for fully dry condition, and the efficiency gain is up to 8% for the fully wet condition.

5. Conclusions

Two-dimensional fin efficiencies of elliptic fins with combined heat and mass transfer have been examined. Some important results and conclusions may be summarized as follows:

1. The temperature profiles are indeed two-dimensional for elliptic fins. The fin temperature distribution is higher as the air relative humidity ϕ is increased. As ϕ is increased, the interface of the fully dry and wet regions moves outward to the elliptic fin tip resulting in the increase of the wet region.
2. The elliptic fin efficiency is increased as the major to minor axis ratio is increased, and the fully wet fin efficiency is lower than that for a dry fin by 10–20%.
3. The conventional 1-D sector method overestimates the elliptic fin efficiency by 0.5–1% as compared to the 2-D analysis.
4. The elliptic fin efficiency is up to 4% higher than the corresponding circular fin efficiencies having the same perimeter for fully dry condition, and the efficiency gain is up to 8% for that of the fully wet condition.

References

[1] F.C. McQuiston, J.D. Parker, in: Heating Ventilating and Air Conditioning Analysis and Design, fourth ed., Wiley, New York, 1994, pp. 604–613.
[2] ARI Standard 410-72, Forced-Circulation Air-Cooling and Air-Heating Coils, Air-Conditioning & Refrigeration Institute, 1972.
[3] J.L. Threlkeld, in: Thermal Environment Engineering, Prentice-Hall, New York, 1970, pp. 257–259.
[4] F.C. McQuiston, Fin efficiency with combined heat and mass transfer, ASHRAE Trans. 71 (1975) 350–355.
[5] J.E.R. Coney, H. Kazeminejad, C.G.W. Sheppard, Dehumidification of air on a vertical rectangular fin: a numerical study, Proc. Inst. Mech. Eng. 203 (1989) 141–146.
[6] J.E.R. Coney, C.G.W. Sheppard, E.A.M. Shafei, Fin performance with dehumidification from humid air: a numerical investigation, Int. J. Heat Fluid Flow 10 (1989) 224–231.
[7] H. Kazeminejad, Analysis of one-dimensional fin assembly heat transfer with dehumidification, Int. J. Heat Mass Transfer 38 (1995) 455–462.
[8] L.T. Chen, Two-dimensional fin efficiency with combined heat and mass transfer between water-wetted fin surface

and moving moist air stream, Int. J. Heat Fluid Flow 12 (1991) 71–76.
[9] A.H. Elmahdy, R.C. Biggs, Efficiency of extended surfaces with simultaneous heat and mass transfer, ASHRAE Trans. 89 (1983) 135–143.
[10] K.T. Hong, R.L. Webb, Calculation of fin efficiency for wet and dry fins, HVAC&R Res. 2 (1996) 27–41.
[11] C.C. Wang, Y.C. Hsieh, Y.T. Lin, Performance of plate finned tube heat exchangers under dehumidifying conditions, J. Heat Transfer 119 (1997) 109–117.
[12] L. Rosario, M.M. Rahman, Overall efficiency of a radial fin assembly under dehumidifying conditions, J. Energy Resour. Technol. 20 (1998) 299–304.
[13] S.Y. Liang, T.N. Wong, G.K. Nathan, Comparison of one-dimensional and two-dimensional models for wet-surface fin efficiency of a plate-fin-tube heat exchanger, Appl. Thermal Eng. 20 (2000) 941–962.
[14] G. Wu, T.Y. Bong, Overall efficiency of a straight fin with combined heat and mass transfer, ASHRAE Trans. Part 1 100 (1995) 367–374.
[15] M.M. Salah El-Din, Performance analysis of partially-wet fin assembly, Appl. Thermal Eng. 18 (1998) 337–349.
[16] L. Rosario, M.M. Rahman, Analysis of heat transfer in a partially wet radial fin assembly during dehumidification, Int. J. Heat Fluid Flow 20 (1999) 642–648.
[17] D. Besendnjak, A. Poredos, Efficiency of cooled extended surfaces, Int. J. Refrig. 21 (1998) 372–380.
[18] H. Brauer, Compact heat exchangers, Chem. Process Eng. 45 (8) (1964) 451–460.
[19] J.Y. Jang, J.Y. Yang, Experimental and numerical analysis of the thermal-hydraulic characteristics of elliptic finned-tube heat exchangers, Heat Transfer Eng. 19 (4) (1998) 55–67.
[20] R.K. Shah, Heat exchanger basic design methods, in: S. Kakac, R.K. Shah, A.E. Bergles (Eds.), Low Reynolds Number Flow Heat Exchanger, Hemisphere, New York, 1983, pp. 21–72.
[21] L.A.O. Rocha, F.E.M. Saboya, J.V.C. Vargas, A comparative study of elliptical and circular sections in one- and two-row tubes and plate fin heat exchangers, Int. J. Heat Fluid Flow 18 (1997) 247–252.
[22] S.M. Saboya, F.E.M. Saboya, Experiments on elliptic sections in one- and two-row arrangements of plate fin and tube heat exchangers, Exp. Thermal Fluid Sci. 24 (2001) 67–75.